Genome evolution in bacteria isolated from million-year-old subseafloor sediment

William D. Orsi[1,2*], Tobias Magritsch[1], Sergio Vargas[1], Ömer K. Coskun[1], Aurele Vuillemin[1], Sebastian Höhna[1,2], Gert Wörheide[1,2,3], Steven D'Hondt[4], B. Jesse Shapiro[5,6,7], Paul Carini[8*]

[1]Department of Earth and Environmental Sciences, Paleontology & Geobiology, Ludwig-Maximilians-Universität München, Richard-Wagner-Strasse 10, 80333 Munich, Germany.

[2]GeoBio-CenterLMU, Ludwig-Maximilians-Universität München, Richard-Wagner-Strasse 10, 80333 Munich, Germany.

[3]SNSB- Bayerische Staatssammlung für Paläontologie und Geologie, Richard-Wagner-Strasse 10, 80333 Munich, Germany.

[4]Graduate School of Oceanography, University of Rhode Island, 215 South Ferry Road, 02882 Narragansett, USA.

[5]Department of Biological Sciences, University of Montreal, QC, Canada

[6]Department of Microbiology and Immunology, McGill University, QC, Canada

[7]McGill Genome Centre, Canada

[8]Department of Environmental Science, the BIO5 Institute, School of Plant Sciences, and the School of Animal & Comparative Biomedical Science, University of Arizona, Tucson, Arizona USA

Corresponding authors*:
Prof. Dr. William D. Orsi
Ludwig-Maximilians-Universität München, Department of Earth and Environmental Sciences, Paleontology & Geobiology, Richard-Wagner-Strasse 10, 80333 Munich, Germany.

Corresponding authors*:
Dr. Paul Carini
Address: University of Arizona, Department of Environmental Science, School of Plant Science, BIO5 Institute. Tucson, Arizona 85721
E-Mail: paulcarini@arizona.edu
Phone/Fax: Phone: 520-621-1646

Running title: Genome evolution in subseafloor bacteria

Keywords: genome evolution; deep biosphere

Significance statement: The nature and extent of genomic evolution in subseafloor microbial populations subsisting for millions of years below the seafloor is unknown. Subseafloor populations have ultra-slow metabolic rates that are hypothesized to restrict reproduction and, consequently, the spread of new traits. Our findings demonstrate that genomes of cultivated bacterial strains from the genus *Thalassospira* isolated from million-year-old abyssal sediment exhibit greatly reduced levels of homologous recombination, elevated numbers of pseudogenes, and genome-wide evidence of relaxed purifying selection. These substitutions and pseudogenes are fixed into the population, suggesting the genome evolution of these bacteria has been dominated by genetic drift, whereby under long-term physical isolation in small population sizes, and in the absence of homologous recombination, newly acquired mutations accumulate in the genomes of clonal populations over millions of years.

Abstract: Beneath the seafloor, microbial life subsists in isolation from the surface world under persistent energy limitation. The nature and extent of genomic evolution in subseafloor microbes has been unknown. Here we show that the genomes of *Thalassospira* bacterial populations cultured from million-year-old subseafloor sediments evolve by point mutation, with a relatively low rate of homologous recombination and a high frequency of pseudogenes. Ratios of synonymous to non-synonymous mutation rates correlate with the accumulation of pseudogenes, consistent with a dominant role for genetic drift in the subseafloor strains, but not in type strains of *Thalassospira* isolated from the surface world. Our findings demonstrate that the long term physical isolation of these bacteria, in the absence of recombination, has resulted in clonal populations that evolve consistent with 'Mullers Ratchet', whereby reduced access to novel genetic material from neighbors has resulted in fixation of new mutations that accumulate in genomes over millions of years.

Main text.

The subseafloor biome contains a large fraction of all prokaryotic cells on Earth totaling circa 10^{29} cells (*1*). This biome subsists over geological timescales under persistent energy limitation (*2-6*). Whether evolution and ecological differentiation occurs in microbial populations below the seafloor has remained controversial. It is generally agreed that extreme energy limitation restricts metabolic activity and growth

68 (*2-6*), which are necessary for new mutations to propagate through populations to foster ecological
69 differentiation and speciation (*7*). However, there has been very little direct examination of this issue at the
70 low metabolic rates and long timescales characteristic of subseafloor life (*8*). Experimental evidence exists
71 for bacterial evolution under energy limitation on laboratory timescales (*9,10*), but a recent metagenomic
72 analysis showed that energy limitation and reduced growth restricted the spread of new mutations through
73 microbial communities over 5,000 years in the upper 2 meters of anoxic sediment from Aarhus Bay
74 (Denmark) (*11*). There have been no direct studies of mutation, homologous recombination, and evolution
75 in microbial communities of the deeper and older sediment that dominates the subseafloor. Here, we used
76 the genomes of bacteria isolated from million-year-old subseafloor abyssal clay sediments to investigate
77 the nature of genome evolution in subseafloor bacteria that persist under extreme energy limitation over
78 long timescales.

79 Newly acquired mutations of functional significance can sweep through relatively fast-growing
80 bacterial populations in surface world habitats and influence ecological differentiation (*12*). However, it is
81 unclear whether such sweeps occur in ancient subseafloor sediment given the comparably slow subseafloor
82 bacterial biomass turnover rates that are estimated to be on thousand-year timescales (*13*). The metabolic
83 rates of microbes persisting in deep-sea abyssal clay are amongst the lowest observed in the subseafloor
84 biosphere, such that these sediments are often oxic through the entire sediment column to the underlying
85 oceanic crust and the microbes live near the low-energy limit to life (*3*,*4*). We cored a 15 m sedimentary
86 sequence of oxygenated abyssal clay at a water depth of 6,000 m in the North Atlantic where the average
87 sedimentation rate is an estimated 1 meter per million years (*14*). Thus, the deepest sediment sampled was
88 deposited ca. 15 million years ago (mya). The relatively slow drawdown of O_2 with increasing depth at
89 this site (Fig. 1A) primarily reflects oxidation of organic matter by aerobic microbes. Abyssal clay is
90 characterized by very low permeability and extremely small pore diameter (*15*), which physically isolates
91 the subseafloor microbial communities from the surface and the microbes within it from each other (see
92 'sediment physical properties' in the SI).

93 We isolated colony-forming bacteria on petri dishes following an 18-month incubation of sediment
94 and sterile ^{18}O-labeled artificial seawater (Fig S1) from 3 and 6 meters below the seafloor (mbsf)(see
95 Methods). Because the mean sedimentation rate is 1 m million yr^{-1}, the age of the sediment horizons from
96 which these bacteria were enriched and isolated are estimated to be 3 and 6 million years old, respectively.
97 The full-length 16S rRNA gene sequences from the isolates had closest similarity (90-99% sequence
98 identity) to the Alphaproteobacteria *Thalassospira xiamenensis and Thalassospira lohafexi* previously
99 isolated from marine surface sediment (*16,17*) and oligotrophic seawater (*18*) (these previously isolated
100 microbes and their related cultured relatives are referred to as 'type strains' herein).

Several lines of evidence indicate the *Thalassospira* isolated from the 3- and 6-mbsf sediment enrichments are endemic to the subseafloor clay and are not a contaminant from the water column or other sources. First, the V4 hypervariable region of the 16S rRNA gene sequences from the sediment slurry enriched *Thalassospira* cultures share >99% sequence identity with an operational taxonomic unit (OTU) previously identified from the *in-situ* community determined from the frozen samples ('OTU_6', Figure 1B,C). This OTU_6 became ^{18}O-labeled during the 18-month enrichment incubation (atomic ^{18}O enrichment of OTU_6 DNA: 59%) in the presence of sterile ^{18}O-labeled seawater (Fig. S1), a proxy for growing microbes (*19*), and had an estimated doubling time in the incubation of 36 ± 1.5 (mean ± SD) days. OTU_6 consists of two amplicon sequence variants (ASVs) that cluster with the *Thalassospira* subseafloor isolates (Otu6_ASV1, Otu6_ASV2), respectively, and are distinguished by a single nucleotide polymorphism (SNP) that is conserved between the ASVs and the subseafloor isolates (Figure 1C). The *in-situ* concentrations of both *Thalassospira* ASVs have highest abundance (ca. 1,000 16S rRNA gene copies g^{-1} sediment) below the seafloor between 4 - 6 mbsf, and both *Thalassospira* ASVs were detected in the 3- and 6-mbsf sediment (Figure 1B). This shows that the *Thalassospira* strains isolated from the 3- and 6-mbsf sediment enrichments are derived from the same distinct 16S rRNA gene ASVs present within the *in-situ* communities. The long-term physical isolation of these isolates in the subseafloor (see 'sediment physical properties' in SI), subsisting under uninterrupted energy limitation within the ancient sediment, provides an opportunity to investigate how the relative effects of recombination, nucleotide substitution, and gene decay have shaped the genomes of the cultivated subsurface *Thalassospira* strains since their burial in the deep-sea clay millions of years ago.

Genome statistics

We sequenced the genomes of ten *Thalassospira* isolates each from the 3- and 6-mbsf sediment enrichments using a hybrid assembly approach consisting of long-read Nanopore sequencing, corrected and polished via short-read Illumina technologies at >100x coverage. The mean genome completeness of these hybrid assemblies is estimated to be 99.7% ± 0.3%; (mean ± SD), with most being 100% complete and representing the complete chromosome (Table S1). The mean length of the new *Thalassospira* genomes is 4.71 ± 0.08 Mbp (mean ± SD), with 4,567 ± 107 (mean ± SD) protein coding genes, and they are assembled to an average of 12 ± 2 (mean ± SD) contigs (Fig. S2 and Table S1). The genome size and the number of protein-encoding genes are similar to those observed within the existing *Thalassospira* type strains isolated from the surface world (Fig. S2).

135 **Core genome phylogenomic analysis**

136 The core genome phylogeny of existing *Thalassospira* type species, and the newly isolated
137 subseafloor *Thalassospira* strains, consists of 1,809 orthologous genes and reveals three clades of
138 subseafloor *Thalassospira*. One clade shares 96-97% genome-wide average nucleotide identity (ANI),
139 and 99.9% 16S rRNA gene sequence identity, with *T. xiamenensis* and *T. permensis* (Fig. S3). We named
140 isolates in this clade *T. xiamenensis* strain 'Neogene', after the Neogene eon (2.8 – 23 mya) which covers
141 both estimated ages of sediment (3 mya and 6 mya) from which the strains in this clade were isolated. The
142 subseafloor genomes in this clade correspond to the 16S rRNA gene ASV1 detected in the *in situ* frozen
143 sediment core samples (Fig 1B, C). A second clade contains three isolates from 6 mbsf sediment shared
144 97% ANI with *T. xiamenensis* and *T. permensis.* Since all isolates in this clade were recovered from ca. 6
145 mya sediment deposited during the Miocene eon (5.33 – 23 mya), we report them as *T. xiamenensis* strain
146 'Miocene' (Fig. S3). However, despite sharing 97% ANI in the core genome with *T. xiamenensis* and *T.*
147 *permensis* (Fig S3), *T. xiamenensis* strain 'Miocene' only shared 90% 16S rRNA gene sequence identity
148 with these closest related type strains. The subseafloor genomes in this clade also correspond to ASV1
149 detected in the *in situ* frozen sediment core samples (Fig 1B, C). A third clade contains subseafloor
150 *Thalassospira* cultures isolated only from 3 mbsf sediment and shares 95-96% ANI with *T. lucentensis*
151 and *T. lohafexi* (Fig. S3). The subseafloor genomes in this clade correspond to the 16S rRNA gene ASV2
152 detected in the *in situ* frozen sediment core samples (Fig 1B,C). Based on the genetic distinctness of
153 these isolates we consider them to be a new candidate species, according to recently provided criteria
154 based on genome-wide ANI (*20*). Because all isolates of this third clade were recovered from 3 mya
155 sediment, we propose the candidate name '*Candidatus* Thalassospira pliocenensis', named after the
156 Pliocene age (2.58 – 5.33 mya) of the deep-sea clay from which they were isolated. Pangenome analysis
157 revealed that flexible genome content is conserved within each of the three subseafloor clades, providing
158 further evidence that each clade represents a genetically distinct population (Fig S4). Laboratory growth
159 rates of the subseafloor *Thalassospira* ranged from 0.064 to 0.31 h^{-1} (Fig. S5).
160
161

162 **Roles of mutation and recombination**

163 The ratio of nucleotide substitutions originating from mutations versus homologous recombination (r/m)
164 can be used to measure the relative effect of homologous recombination on the genetic diversification of
165 populations (*21*). Due to the physical isolation of individual bacterial cells, reduced cell concentrations,
166 and the reduced availability of extracellular DNA for recombination in subseafloor sediments (*22*) we
167 hypothesized that r/m ratios would be lower in the subseafloor *Thalassospira* populations than in the type
168 strains. To test this, we used an established method (*23*) to calculate the relative rate of recombination to

169 mutation (R/θ), the mean length of recombined DNA (δ), and the mean divergence of imported DNA (v)
170 for branch tips (existent genomes) and internal nodes (ancestral states) in the *Thalassospira* core genome
171 phylogeny, which allows for a calculation of r/m (r/m = $(R/\theta) * \delta * v$). This analysis showed that in the
172 *Thalassospira* core genome, the r/m is approximately ten times lower in the subseafloor core genome (r/m
173 = 0.078) than in the type strains (r/m = 0.71) (Table 1), indicating that homologous recombination plays a
174 much lesser role in the diversification of the subseafloor strains. The r/m values of the subseafloor
175 *Thalassospira* are furthermore anomalously low compared to free-living bacteria isolated from the surface
176 world, which have r/m values that range from 0.1-64 (*21*). Concomitant with the ten-fold lower r/m values
177 compared to the type strains (Table 1), the subseafloor *Thalassospira* core genomes exhibit far fewer
178 numbers of inferred imported DNA from recombination events compared to the *Thalassospira* type strains
179 and the ancestral states of the last common ancestors shared with the type strains (Fig. 2).
180 The ancestral recombination signal is not preserved in the genomes of the subseafloor isolates (Fig.
181 2), which is consistent with a shift away from a recombination-influenced population toward a more clonal
182 population structure since the subseafloor *Thalassospira* diverged away from the last common ancestor
183 shared with the type strains. We looked for evidence of evolution by investigating pairwise substitution
184 numbers in the subseafloor *Thalassospira* genomes. We identified tens to thousands of nucleotide
185 differences (single nucleotide polymorphisms [SNPs]) within each subseafloor *Thalassospira* clade (Fig
186 S6). The SNPs in subseafloor *Thalassospira* strains were present in a clade-specific manner (Fig S7). But,
187 while the precise SNPs are clade-specific, the SNPs occurred in genes coding for related functions across
188 different clades. These included genes with predicted annotations involved in flagellar motility (FlhB,
189 FliO), transcription (TetR and Fis family transcriptional regulators), cell wall biogenesis (peptidase S41,
190 peptidoglycan DD-metalloendoptidase M23), and transport and metabolism of amino acids and
191 carbohydrates (Fig. S7).
192 We considered that the observed nucleotide substitutions occurred within the subseafloor
193 populations during the culture enrichment and cultivation process. However, the measured generation times
194 of the *Thalassospira* (OTU6) in the incubation measured with qPCR (36 ± 1.5 days; mean ± SD) indicate
195 an estimated maximum of 15 doublings over the enrichment (see SI). At common bacterial mutation rates
196 of 10^{-9} to 10^{-10} mutations bp^{-1} $generation^{-1}$ (*24*), more than 4,000 generations would be required to obtain
197 the observed nucleotide diversity present in the subsurface *Thalassospira* genomes (Fig. S8). Thus, newly
198 accumulated mutations in culture are insufficient to explain the observed interpopulation nucleotide
199 diversity between the subseafloor genomes (Fig. S8). The inter-population nucleotide diversity of the
200 subseafloor strains therefore arose during their long-term subsistence in the ancient sediments and is not
201 the result of evolution during the laboratory incubation.
202

203 **Substitutions and pseudogenes are fixed in subseafloor populations**

204 Compared to the type strains, the subseafloor *Thalassospira* genomes exhibit higher numbers of
205 pseudogenes (non-functional parts of the genome that resemble functional genes), and non-synonymous
206 substitutions (substitutions that alter the amnio acid sequence of a protein). We identified 47.9 ± 8.57 (mean
207 ± SD) pseudogenes in the genomes of subseafloor *Thalassospira* isolates, which is significantly higher than
208 the number of pseudogenes identified in the type strains (22.1 ± 5.52 pseudogenes [mean ± SD]; Table 1,
209 Figure 3, and Fig. S2) (two-sided T-test: P=1.5E-10). Similarly, we observed a modest but significant
210 elevation of genome-wide nonsynonymous to synonymous substitution rates (dN/dS) in the genomes of the
211 subseafloor *Thalassospira* strains (0.035 ± 0.006; mean ± SD), relative to the type strains (0.022 ±0.012;
212 mean ± SD) (two-sided t-test P=0.0002; Table 1, Figure 3 and Fig. S2). Similar to the SNPs (Fig. S7), the
213 composition of pseudogenes occurred in a clade-specific manner (ANOSIM: P = 0.001) (Fig S9). Compared
214 to the type strains, the predicted annotations of the pseudogenes in the subseafloor *Thalassospira* genomes
215 are skewed toward those involved in transcription, energy conservation, amino acid and carbohydrate
216 metabolism, and flagellar motility (Fig S9). Moreover, subseafloor genomes have significantly higher
217 numbers of pseudogenes involved in motility (flagellar biosynthesis genes: FliN, FliK, FlhO) compared to
218 the type strains (two-sided t-test: *P*=0.003) (Fig S10).

219 The elevated and correlated dN/dS ratios and proportion of pseudogenes for these isolates (Fig. 3)
220 is a hallmark of Muller's ratchet (*24-28*) and is a further indication that the three clades of subsurface
221 *Thalassospira* are clonal and unable to eliminate deleterious mutations that otherwise would be purged
222 from natural populations that are able to freely recombine. Burial in the sediment millions of years ago
223 resulted in physical isolation of subsurface *Thalassospira* cells and was the impetus for a transition from
224 freely recombining populations to recombination-limited clonal populations that rarely encounter
225 genetically diverse recombination partners that introduce genetic diversity into the population.
226 Simultaneously, the effective population sizes of subsurface *Thalassospira* were restricted by the very low
227 flux of bioavailable energy in subseafloor sediment. The reduced energy flux limited the environmental
228 carrying capacity (*1*), and thus the *Thalassospira* population size, in this ancient subseafloor clay. The lack
229 of available energy also likely significantly reduced the potential for cellular motility (*5, 22*). The combined
230 effects of physical isolation, low cell concentrations, and little or no motility, resulted in the further
231 reduction of recombination events due to infrequent cell-cell contact. The reduction of homologous
232 recombination resulted in mutation becoming the dominant driver of evolution in these clonal subseafloor
233 *Thalassospira* populations (Table 1), leading to relaxed purifying selection in the absence of recombination.
234 Although we see elevated dN/dS ratios and an accumulation of pseudogenes across the genomes of
235 subsurface *Thalassospira* (Fig. 3), some functions appear to be more prone to gene decay than others. For
236 example, genes predicted to be involved in flagellar motility were present in both the SNP (*fliO*, *flhB*, *flgH*;

Fig. S7) and pseudogene (*fliN*, *fliK*, *flhO*; Fig. S9, S10) analysis, suggesting flagellar motility may become a non-essential trait (*5, 22*) subject to purifying relaxed selection in abyssal clay with (which is characterized by very low permeability and extremely small pore diameter, despite its high porosity [*15*]). Finally, the accumulation of mutations via Muller's ratchet (*24*) may explain the reduced growth rates (29) of the subsurface *Thalassospira*, relative to the type strains (Fig. S5).

Outlook:

Our findings demonstrate that subseafloor *Thalassospira* genomes analyzed here have evolved akin to endosymbiotic bacteria, whereby clonal populations also lack homologous recombination and are thus subject to genetic drift whereby deleterious mutations become fixed and Muller's Ratchet (*24*) eventually leads to the extinction of endosymbiotic bacterial lineages (*25*). Our genomes show similar signs of evolution, but dN/dS ratios observed in the subseafloor *Thalassospira* genomes are lower than those seen in endosymbiotic bacteria (*28*) and genome reduction was absent. This could be explained by the subseafloor genomes experiencing a single bottleneck in the form of a burial event followed by a stable but low population size, in contrast to the repeated population bottlenecks experienced by endosymbionts at each insect generation.

Subseafloor cell concentrations are low and decrease substantially with increasing depth (*1*). Because genetic drift has a stronger effect on populations with small population sizes (*25*,*28*), physically isolated microbes experiencing clonal growth and reduced homologous recombination in the deep biosphere may be particularly prone to genetic drift-mediated evolution. Because the subseafloor biosphere contains a large fraction of all bacterial cells on Earth (*1*), our findings suggest drift-like evolutionary processes in the absence of homologous recombination may be much more widely distributed in nature than previously thought. Future assessments of homologous recombination and drift in single cell genomes from uncultured lineages of bacteria and archaea that comprise most subsurface energy limited communities (*30)* could be used to assess how widespread this evolutionary mechanism is within the subsurface biosphere.

Acknowledgements. This work was supported primarily by the Deutsche Forschungsgemeinschaft (DFG) project OR 417/1-1 granted to W.D.O. Publication of the manuscript was supported by the LMU Mentoring Program. The expedition was funded by the US National Science Foundation through grant NSF-OCE-1433150 to S.D. This is Center for Dark Energy Biosphere Investigations (C-DEBI) publication number XXX. A portion of this work was performed as part of the LMU Masters Program "Geobiology and Paleobiology" (MGAP). P.C. was supported by the University of Arizona's Technology and Research

Initiative Fund (the Water, Environmental, and Energy Solutions initiative). We thank William F. Martin for comments on the manuscript.

Author contributions. W.D.O., P.C., J.S., and G.W. conceived the work and experimental approach. W.D.O., T.M., O.K.C., S.V., P.C., S.H., and A.V. contributed to the laboratory and bioinformatics analyses and experimental work. S.D. provided the samples from the KN223 R/V Knorr oceanographic expedition KN223. All authors discussed and wrote the manuscript and commented on the paper.

Competing interests. The authors declare that they have no competing interests.

Supplemental information. Supplemental Table 1, Supplemental Figures S1-S10, References 31-49.

Data and materials availability. Data are publicly available through NCBI BioProject PRJNA473406. The raw genomic sequences reads and genome assemblies are available in SRA BioSample accessions SAMN17168194, SAMN17168195, and SAMN17168196. The 16S data from the frozen core are available in SRA BioSample accessions SAMN10929403 to SAMN10929517. Figures and output files from the pangenomic analysis in Anvio are available online through FigShare (https://doi.org/10.6084/m9.figshare.13372619). Additional data related to this paper may be requested from the authors.

References

1. J. Kallmeyer, R. Pockalny, R. R. Adhikari, D. C. Smith, S. D'Hondt, Global distribution of microbial abundance and biomass in subseafloor sediment. *Proc Natl Acad Sci U S A* **109**, 16213-16216 (2012).
2. S. D'Hondt, S. Rutherford, A. J. Spivack, Metabolic activity of subsurface life in deep-sea sediments. *Science* **295**, 2067-2070 (2002).
3. S. D'Hondt *et al.*, Subseafloor sedimentary life in the South Pacific Gyre. *Proc Natl Acad Sci U S A* **106**, 11651-11656 (2009).
4. H. Roy *et al.*, Aerobic microbial respiration in 86-million-year-old deep-sea red clay. *Science* **336**, 922-925 (2012).
5. T. M. Hoehler, B. B. Jorgensen, Microbial life under extreme energy limitation. *Nat Rev Microbiol* **11**, 83-94 (2013).
6. S. D'Hondt, G. Wang, A. Spivack, The underground economy (Energentic Constraints of Subseafloor Life). Chapter 2.3 in "Earth and Life Processes Discovered from Subseafloor Environment – A Decade of Science Achieved by the Integrated Ocean Drilling Program (IODP)" R. Stein, D. Blackman, F. Inagaki, H. -C. Larson Eds. Pages 127-148. Elsevier, Amsterdam/New York (2014).
6. D'hondt 2014
7 O. X. Cordero, M. F. Polz, Explaining microbial genomic diversity in light of evolutionary ecology. *Nat Rev Microbiol* **12**, 263-273 (2014).
8. J. F. Biddle *et al.*, Prospects for the study of evolution in the deep biosphere. *Front Microbiol* **2**, 285 (2012).

9. S. E. Finkel, Long-term survival during stationary phase: evolution and the GASP phenotype. *Nat Rev Microbiol* **4**, 113-120 (2006).
10. L. M. Wick, H. Weilenmann, T. Egli, The apparent clock-like evolution of Escherichia coli in glucose-limited chemostats is reproducible at large but not at small population sizes and can be explained with Monod kinetics. *Microbiology (Reading)* **148**, 2889-2902 (2002).
11. P. Starnawski *et al.*, Microbial community assembly and evolution in subseafloor sediment. *Proc Natl Acad Sci U S A* **114**, 2940-2945 (2017).
12. B. J. Shapiro *et al.*, Population genomics of early events in the ecological differentiation of bacteria. *Science* **336**, 48-51 (2012).
13. B. A. Lomstein, A. T. Langerhuus, S. D'Hondt, B. B. Jorgensen, A. J. Spivack, Endospore abundance, microbial growth and necromass turnover in deep sub-seafloor sediment. *NAture* **484**, 101-104 (2012).
14. A. Vuillemin *et al.*, Archaea dominate oxic subseafloor communities over multimillion-year time scales. *Sci Adv* **5**, eaaw4108 (2019).
15. Y. Morono, *et al.* Aerobic microbial life persists in oxic marine sediment as old as 101.5 million years, *Nature Communications* **11**, 3626, (2020).
16. M. Li, S. Yang, Q. Lai, Z. Shao, Draft Genome Sequence of Thalassospira xiamenensis Strain MCCC 1A03042(T). *Genome Announc* **5**, (2017).
17. C. Liu, Y. Wu, L. Li, Y. Ma, Z. Shao, Thalassospira xiamenensis sp. nov. and Thalassospira profundimaris sp. nov. *Int J Syst Evol Microbiol* **57**, 316-320 (2007).
18. A. Hutz, K. Schubert, J. Overmann, Thalassospira sp. isolated from the oligotrophic eastern Mediterranean Sea exhibits chemotaxis toward inorganic phosphate during starvation. *Appl Environ Microbiol* **77**, 4412-4421 (2011).
19. B. A. Hungate *et al.*, Quantitative microbial ecology through stable isotope probing. *Appl Environ Microbiol* **81**, 7570-7581 (2015).
20. L. M. Rodriguez-R, K. Konstantinidis, Bypassing cultivation to identify bacterial species. *Microbe* **9**, 111-118 (2014).
21. M. Vos, X. Didelot, A comparison of homologous recombination rates in bacteria and archaea. *ISME J* **3**, 199-208 (2009).
22. M. A. Lever *et al.*, Life under extreme energy limitation: a synthesis of laboratory- and field-based investigations. *FEMS Microbiol Rev* **39**, 688-728 (2015).
23. X. Didelot, D. J. Wilson, ClonalFrameML: efficient inference of recombination in whole bacterial genomes. *PLoS Comput Biol* **11**, e1004041 (2015).
24. J. W. Drake, B. Charlesworth, D. Charlesworth, J. F. Crow, Rates of spontaneous mutation. *Genetics* **148**, 1667-1686 (1998).
24 H. J. Muller, The relation of recombination to mutational advance. *Mutat Res* **106**, 2-9 (1964).
25. J. P. McCutcheon, N. A. Moran, Extreme genome reduction in symbiotic bacteria. *Nat Rev Microbiol* **10**, 13-26 (2011).
26. H. Ochman, L. M. Davalos, The nature and dynamics of bacterial genomes. *Science* **311**, 1730-1733 (2006).
27. N. A. Moran, Accelerated evolution and Muller's rachet in endosymbiotic bacteria. *Proc Natl Acad Sci U S A* **93**, 2873-2878 (1996).
28. C. H. Kuo, N. A. Moran, H. Ochman, The consequences of genetic drift for bacterial genome complexity. *Genome Res* **19**, 1450-1454 (2009).
29. D. I. Andersson, D. Hughes, Muller's rachet decreases fitness of a DNA-based microbe. *Proc Natl Acad Sci U S A* **93**, 906-907 (1996).
30. K. G. Lloyd, A. D. Steen, J. Ladau, J. Yin, L. Crosby, Phylogenetically Novel Uncultured Microbial Cells Dominate Earth Microbiomes. *mSystems* **3**, (2018).

364 **Figure legends**

365

366 **Figure 1: Isolated subsurface *Thalassospira* are most abundant at 3-7 mbsf and distinct from**
367 **related type strains isolated from overlying water and sediments.** (A) Vertical profile of total 16S
368 rRNA gene concentrations determined via qPCR (squares), and oxygen concentrations (circles). 16S
369 rRNA gene concentration points are the average abundances of three technical qPCR replicates with
370 ranges shown with error bars. (B) qPCR-normalized average concentrations of the *Thalassospira*
371 affiliated 'Otu6' ASVs. Error bars are ranges from three technical qPCR replicates. Asterisks mark the
372 depths for the long term ^{18}O-water incubation experiments, enrichments, and cultivation. (C) Maximum
373 likelihood (PhyML) phylogenetic analysis of the *Thalassospira* 16S rRNA gene ASVs (V4 hypervariable
374 region), together with subseafloor and type strain *Thalassospira* 16S rRNA gene V4 regions. The
375 presence of the SNP is displayed. Black, grey, and white dots at the nodes represent >90%, >70%, >50%
376 bootstrap support, respectively.

377 **Figure 2: Recombination in the conserved core genome is limited in subseafloor *Thalassospira***
378 **populations.** The maximum likelihood (PhyML) phylogenetic tree is based on a concatenated alignment
379 of 1,809 genes conserved across all *Thalassospira* genomes ('core genes'). Black circles on nodes
380 represent bootstrap values >95%. The position of recombination events in the core genome are
381 represented by dark blue dots. Positions of low nucleotide diversity and no recombination events in the
382 core genome are shown in light blue. Nucleotide diversity at specific sites in the core genome are
383 illustrated with a color gradient (white: less diversity, orange: more diversity). Histograms on the right
384 display the total number of recombination events (imports) in each genome sequence, and ancestral state
385 reconstructions (internal nodes), as detected by ClonalFrameML (*23*).

386 **Figure 3: The number of pseudogenes and dN/dS ratios are elevated and correlated in subseafloor**
387 ***Thalassospira* populations.** Subseafloor genomes accumulate more pseudogenes as a function of
388 increasing dN/dS ratios compared to the type strains. Linear regressions for type strains, subseafloor
389 strains, and all strains are displayed.

390 **Table 1. The contributions of recombination and mutation to nucleotide diversity in subseafloor**
391 **populations.** The results from ClonalFrameML (*23)* analysis used to calculate the relative contributions
392 of recombination and mutation in the core genome (r/m). *R/θ*: the relative rate of recombination
393 compared to mutation, *δ*: the average length of recombined (imported) DNA, *v*: mean divergence of
394 imported DNA. Also displayed are the average number of pseudogenes and dN/dS ratios (+/- standard
395 deviation). ** two sided T-test: P = 0.005. *****two sided T-test: P = 0.000001.

Figure 1

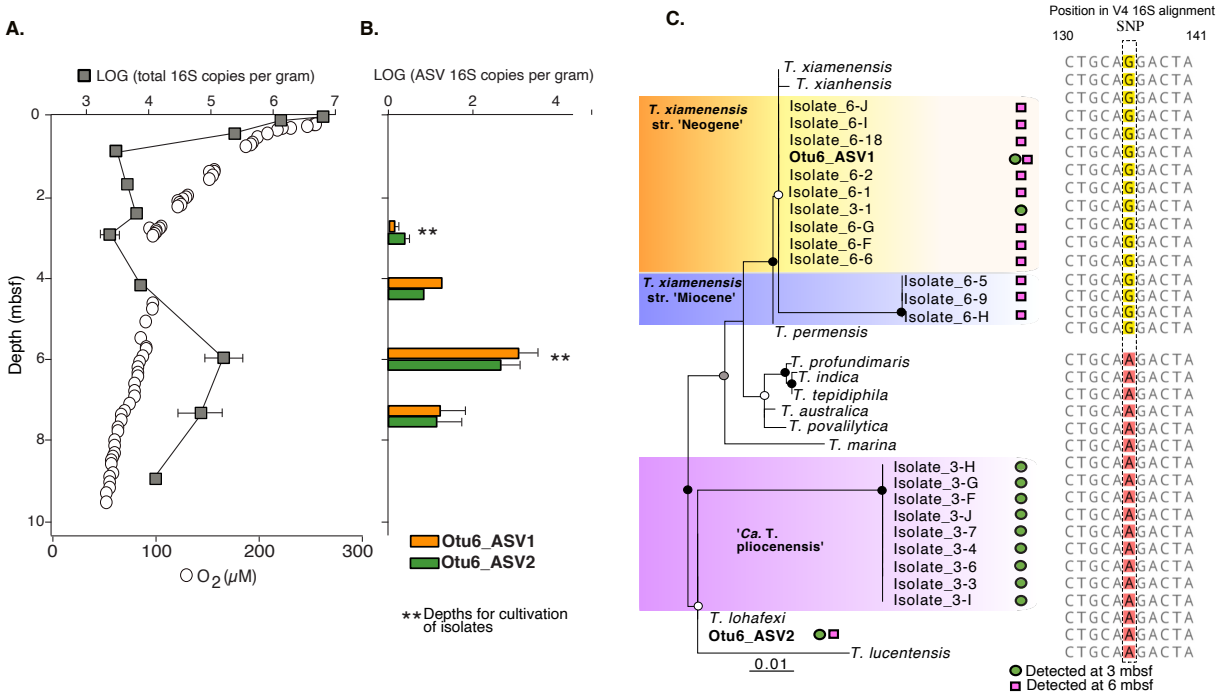
A.
LOG (total 16S copies per gram)
Depth (mbsf)
O2 (μM)
B.
LOG (ASV 16S copies per gram)
Otu6_ASV1
Otu6_ASV2
**Depths for cultivation of isolates
C.
Position in V4 16S alignment
SNP
T. xiamenensis
T. xianhensis
T. xiamenensis str. 'Neogene'
T. xiamenensis str. 'Miocene'
Otu6_ASV1
Otu6_ASV2
T. permensis
T. profundimaris
T. indica
T. tepidiphila
T. australica
T. povalilytica
T. marina
'Ca. T. pliocenensis'
T. lohafexi
T. lucentensis
0.01
Detected at 3 mbsf
Detected at 6 mbsf

Table 1

Group	# strains	*R/θ*	*δ*	*v*	r/m	# pseudogenes	dN/dS
All subseafloor and type strains	34	0.053	244	0.055	0.71	37 (+/- 8)	0.025 (+/- 0.011)
Type strains	13	0.04	333	0.053	0.71	21 (+/- 3)	0.022 (+/- 0.01)
Subseafloor	21	0.006	500	0.026	0.078	48 (+/- 4)****	0.038 (+/- 0.007)**

Figure 2

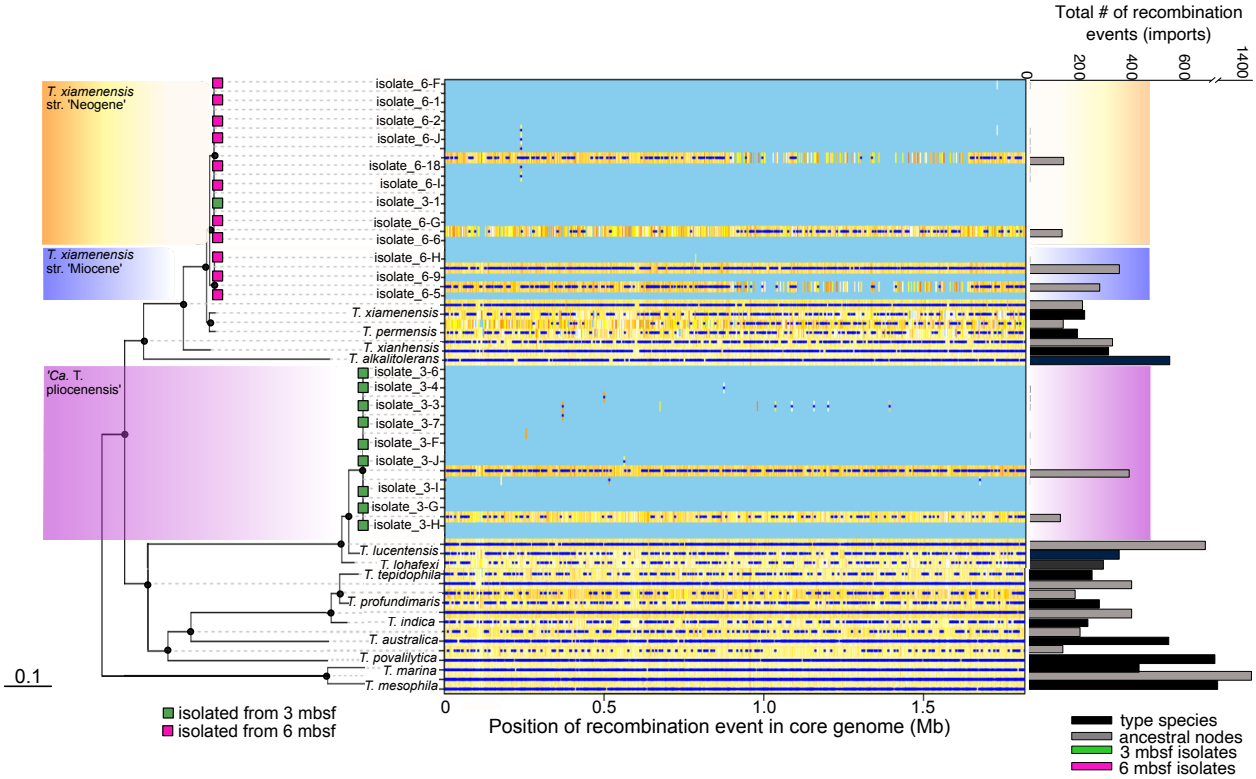

429
430
431
432
433
434 **Figure 3**
435

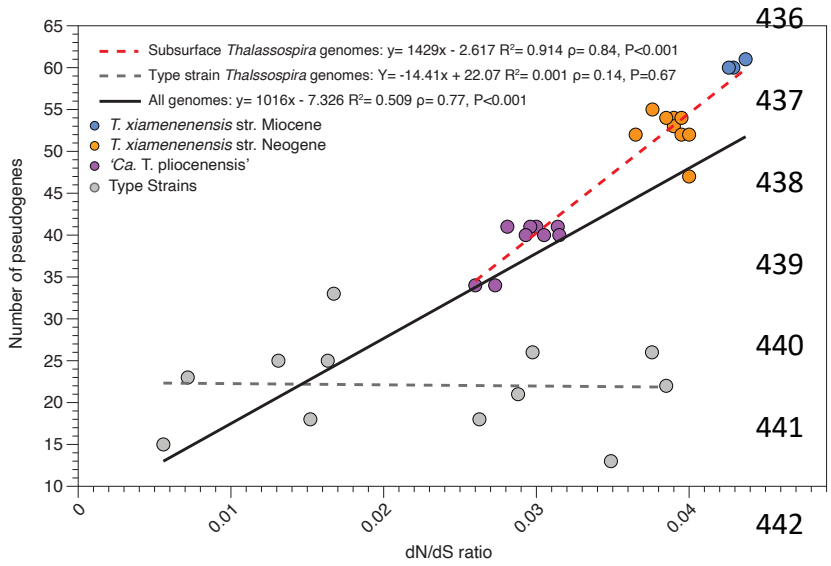

436
437
438
439
440
441
442
443
444
445
446
447
448
449

Supplemental Information

Genome evolution in bacteria isolated from million-year-old subseafloor sediments

William D. Orsi[1,2*], Tobias Magritsch[1], Sergio Vargas[1], Ömer K. Coskun[1], Aurele Vuillemin[1], Sebastian Höhna[1,2], Gert Wörheide[1,2,3], Steven D'Hondt[4], B. Jesse Shapiro[5,6,7], Paul Carini[8*]

[1]Department of Earth and Environmental Sciences, Paleontology & Geobiology, Ludwig-Maximilians-Universität München, Richard-Wagner-Strasse 10, 80333 Munich, Germany.

[2]GeoBio-CenterLMU, Ludwig-Maximilians-Universität München, Richard-Wagner-Strasse 10, 80333 Munich, Germany.

[3]SNSB- Bayerische Staatssammlung für Paläontologie und Geologie, Richard-Wagner-Strasse 10, 80333 Munich, Germany.

[4]Graduate School of Oceanography, University of Rhode Island, 215 South Ferry Road, 02882 Narragansett, USA.

[5]Department of Biological Sciences, University of Montreal, QC, Canada

[6]Department of Microbiology and Immunology, McGill University, QC, Canada

[7]McGill Genome Centre, Canada

[8]Department of Environmental Science, the BIO5 Institute, School of Plant Sciences, and the School of Comparative Animal & Biomedical Science, University of Arizona, Tucson, Arizona USA

479 **Table S1. Genome summary statistics.**

480

Group	isolation depth	isolate	N50 contig size (bp)	size (Mb)	# contigs	GC content	completeness (CheckM)	Contamination (CheckM)	predicted genome size (Mb)	# PEGs	Predicted #f PEGs	% core genome
Ca. T. pliocenensis'	3 mbsf	3.4	649,568	4.7	13	53.5	100%	0%	4.7	4463	4463	40.5
		3.7	1,392,694	4.73	13	53.5	100%	0%	4.73	4463	4463	40.5
		3.F	1,049,738	4.64	13	53.5	100%	0%	4.64	4463	4463	40.5
		3.G	1,232,970	4.64	13	53.5	100%	0%	4.64	4463	4463	40.5
		3.H	994,209	4.64	13	53.5	100%	0%	4.64	4463	4463	40.5
		3.I	735,219	4.64	11	53.5	100%	0%	4.64	4466	4466	40.5
		3.J	1,232,974	4.64	11	53.5	100%	0%	4.64	4466	4466	40.5
		3.3	556,527	4.64	13	53.5	100%	0%	4.64	4463	4463	40.5
		3.6	1,047,050	4.63	13	53.5	100%	0%	4.63	4463	4463	40.5
T. xiamenensis 'Neogene'	6 mbsf	6.1	823,074	4.74	10	54.8	99.50%	0%	4.76	4651	4674	38.9
		6.2	671,859	4.59	9	54.8	97%	0%	4.73	4481	4620	40.4
		6.6	1,045,808	4.74	12	54.8	100%	0%	4.74	4622	4622	39.1
		6.18	1,220,195	4.75	14	54.8	100%	0%	4.75	4651	4651	38.9
		6.F	1,372,017	4.74	9	54.8	99.50%	0%	4.76	4637	4660	39.0
		6.G	1,372,000	4.73	7	54.8	99.50%	0%	4.75	4636	4659	39.0
		6.I	1,156,923	4.75	11	54.8	100%	0%	4.75	4651	4651	38.9
		6.J	1,392,823	4.64	8	54.8	98%	0%	4.76	4555	4672	39.7
	3 mbsf	3.1	1,245,526	4.75	12	54.8	100%	0%	4.75	4673	4673	38.7
T. xiamenensis 'Miocene'	6 mbsf	6.5	484,976	4.87	16	54.7	100%	0%	4.87	4730	4730	38.2
		6.9	484,974	4.87	15	54.7	100%	0%	4.87	4728	4728	38.3
		6.H	484,664	4.87	16	54.6	100%	0%	4.87	4732	4732	38.2

481

482

483

484

485

486

487

488

489

490

491

492

493

494

495

496

497

498

499

500

501

Figure S1. Top panel: ^{18}O-labeling of 16S rRNA genes from the *Thalassospira* OTU6 (see Figure 1), after 7 and 18 months of incubation with ^{18}O-labeled water from the 3 mbsf sediment (data originally published in Vuillemin et al., 2019). **Middle panel:** Oxygen consumption over time in the 18 month slurry from the 3 mbsf incubation (filled circles), and slurries containing labeled water and autoclaved sediment (killed control). **Bottom photo**: cultivation of colony forming bacteria on solid media after the 18 month incubation of sediment slurries in sterile ^{18}O-labeled artificial sea water. No bacterial colonies formed on petri dishes that were inoculated with the killed control slurries.

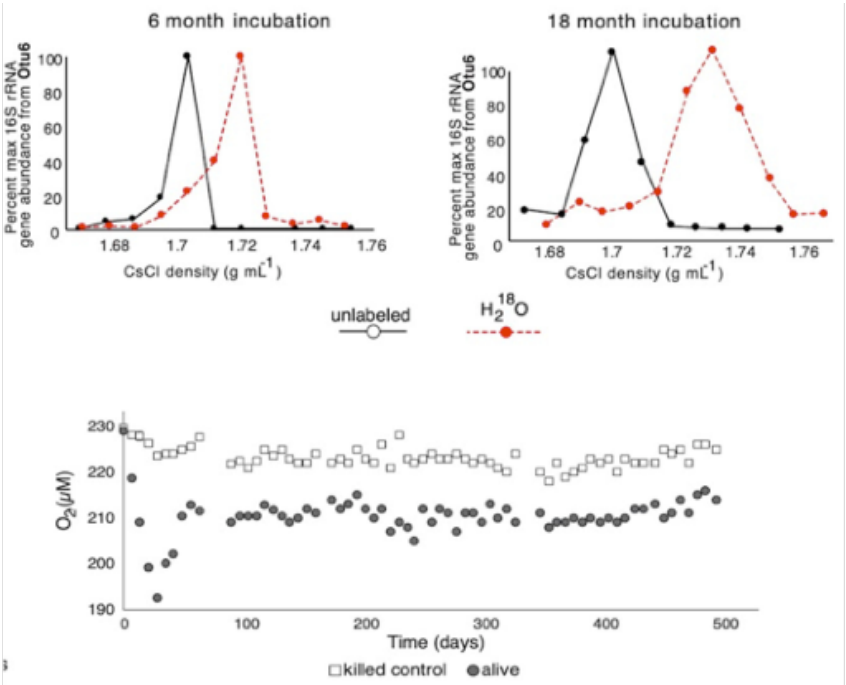

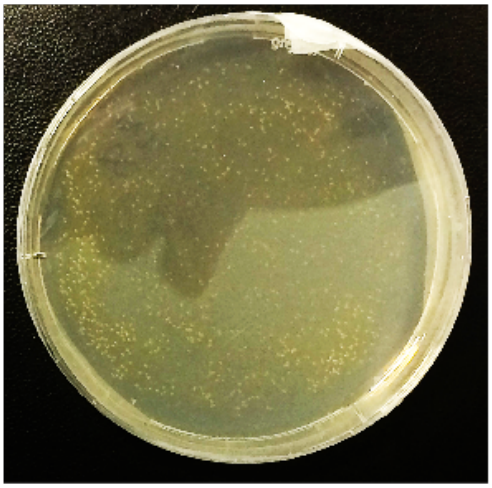

527 **Figure S2: Summary of genome properties for *Thalassospira* strains used in this study.**
528 Points are derived from the analysis of existing genome sequences (for "Type" strains), and new
529 high-quality draft genomes sequenced as part of this study. Box plots illustrate interquartile
530 range ± 1.5 × interquartile range. The horizontal line in each box plot is the median.
531

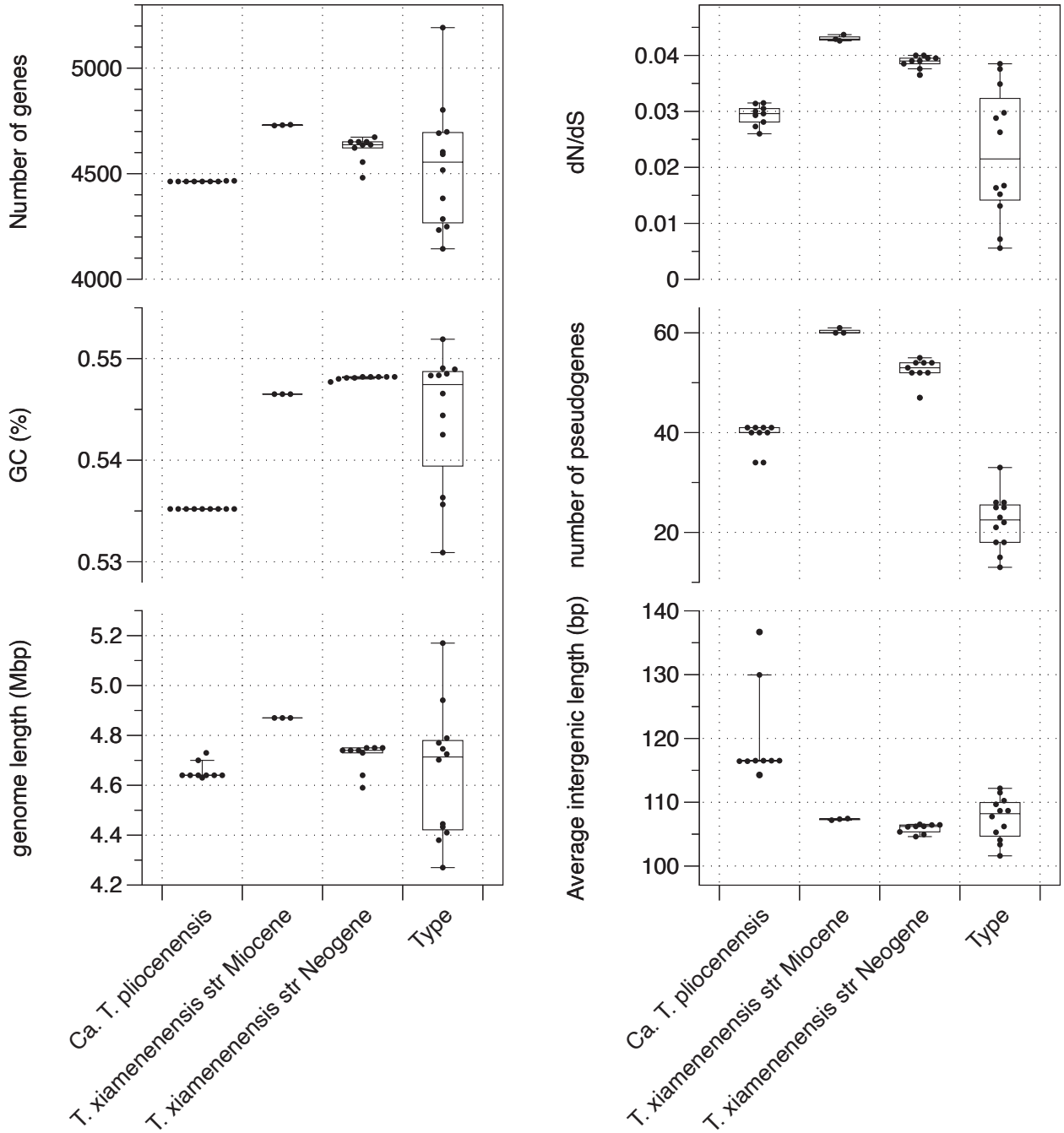

532

533

534

535 **Figure S3. Average nucleotide identity (ANI) and the core genome phylogeny.** The tree is
536 based on maximum likelihood and a concatenated alignment of 1,809 core genes
537

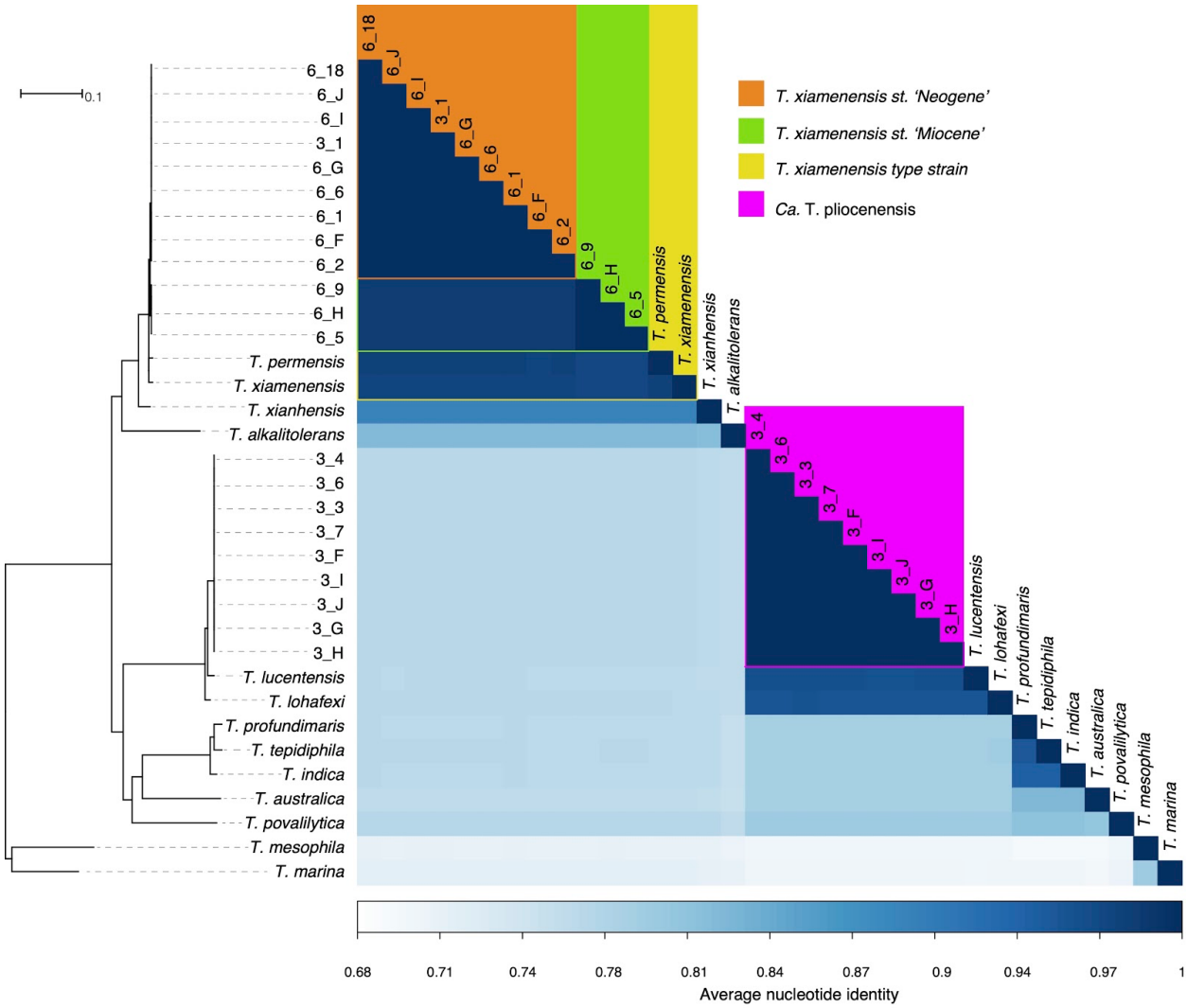

538
539
540
541
542
543
544
545

Figure S4: Pangenome analysis of all *Thalassospira* genomes included in the study. The internal dendrogram is a UPGMA based on the presence/absence of shared gene orthologs. Black bars in the first (inner) 34 circles show the occurrence of gene clusters in the genome of *Thalassospira* species. Grey areas and light colors in the circles represent gene clusters that were detected in the corresponding genome. The next eight bars show statistics for the pangenome analysis of each individual gene cluster (inner circle to outer circle) # contributing genomes: # of genomes that has a hit in a gene cluster, (GC), max # paralogs, single copy gene clusters (SCG), Functional Homogeneity index, Geometric homogeneity index, combined homogeneity index, presence of a COG functional assignment. The categories on the right side (below dendrogram) show the totals per genome for # of gene clusters found in each genome, Num genes per kbp: Number of genes per kilobase pairs of genome. Redundancy: Multiple occurrence of single copy genes in a genome, Completeness: Calculated from the occurrences of single copy gene set in a genome

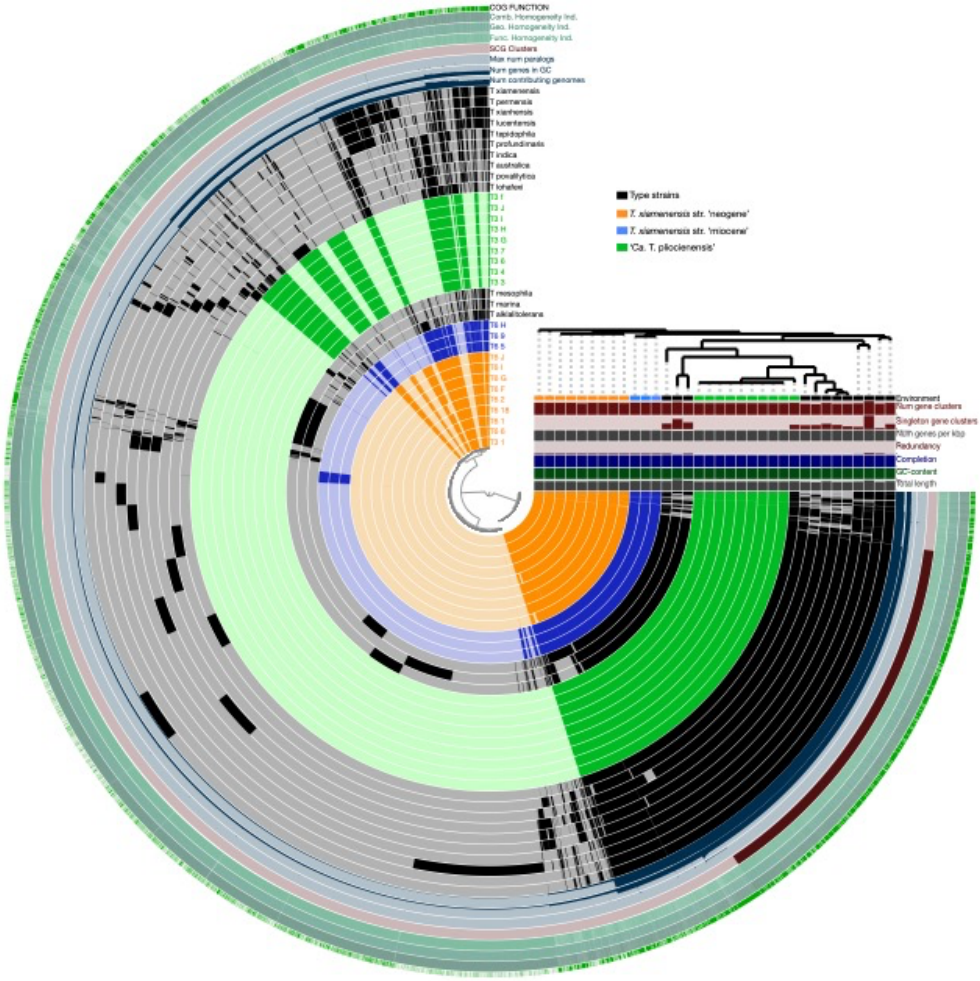

Figure S5. Laboratory growth rates of subsurface *Thalassospira* isolates in comparison to type strain *T. xiamenenensis*. Box plots illustrate interquartile range ± 1.5 × interquartile range. The horizontal line in each box plot is the median. For subsurface strains, growth rates were calculated for each strain across three independent experiments. For the *T. xiamenenesis* type strain, growth rates were calculated from triplicate flasks of one experiment.

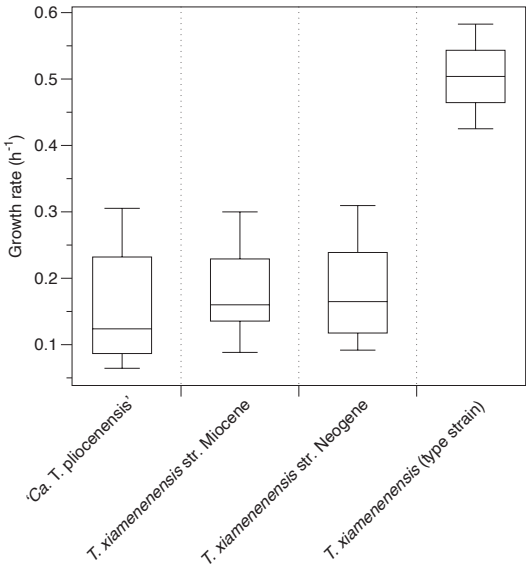

Figure S6. The number of SNPs between pairs of subseafloor *Thalassospira* genomes.

		'Ca. T. pliocienensis'									*T. xiamenensis* str. 'Miocene'			*T. xiamenensis* str. 'Neogene'								
		3_3	3_4	3_6	3_7	3_F	3_G	3_H	3_I	3_J	6_9	6_5	6_H	3_1	6_1	6_2	6_6	6_G	6_18	6_F	6_I	6_J
'Ca. T. pliocienensis'	3_3		225	206	240	226	239	239	695	698	403,756	403,358	403,350	403,126	402,924	403,920	403,178	402,966	403,318	403,762	403,239	403,517
	3_4	225		21	55	73	94	94	550	569	403,771	403,374	403,365	403,140	402,939	403,935	403,193	402,981	403,333	403,776	403,253	403,532
	3_6	206	21		34	52	73	73	529	548	403,764	403,367	403,358	403,133	402,932	403,928	403,186	402,974	403,326	403,769	403,246	403,525
	3_7	240	55	34		18	39	39	495	514	403,768	403,371	403,362	403,137	402,936	403,932	403,190	402,978	403,330	403,773	403,250	403,529
	3_F	226	73	52	18		21	21	477	500	403,760	403,363	403,354	403,129	402,928	403,924	403,182	402,970	403,322	403,765	403,242	403,521
	3_G	239	94	73	39	21		0	456	479	403,758	403,361	403,352	403,126	402,925	403,921	403,179	402,967	403,319	403,762	403,239	403,518
	3_H	239	94	73	39	21	0		456	479	403,758	403,361	403,352	403,126	402,925	403,921	403,179	402,967	403,319	403,762	403,239	403,518
	3_I	695	550	529	495	477	456	456		23	403,864	403,467	403,458	403,230	403,029	404,025	403,283	403,071	403,423	403,866	403,343	403,622
	3_J	698	569	548	514	500	479	479	23		403,863	403,466	403,457	403,229	403,028	404,024	403,282	403,070	403,422	403,865	403,342	403,621
T. xiamenensis str. 'Miocene'	6_9	403,756	403,771	403,764	403,768	403,760	403,758	403,758	403,864	403,863		1,071	909	29,065	29,754	30,305	29,775	29,461	29,826	30,652	29,952	29,949
	6_5	403,358	403,374	403,367	403,371	403,363	403,361	403,361	403,467	403,466	1,071		720	29,269	29,485	30,167	29,686	29,156	29,425	30,749	30,145	29,710
	6_H	403,350	403,365	403,358	403,362	403,354	403,352	403,352	403,458	403,457	909	720		28,731	29,354	30,138	29,555	29,127	29,294	30,102	29,498	29,579
T. xiamenensis str. 'Neogene'	3_1	403,126	403,140	403,133	403,137	403,129	403,126	403,126	403,230	403,229	29,065	29,269	28,731		1,465	2,239	1,547	1,128	1,380	2,084	1,461	1,683
	6_1	402,924	402,939	402,932	402,936	402,928	402,925	402,925	403,029	403,028	29,754	29,485	29,354	1,465		2,232	760	1,213	1,245	2,132	924	1,038
	6_2	403,920	403,935	403,928	403,932	403,924	403,921	403,921	404,025	404,024	30,305	30,167	30,138	2,239	2,232		2,452	2,101	2,103	3,602	2,646	2,394
	6_6	403,178	403,193	403,186	403,190	403,182	403,179	403,179	403,283	403,282	29,775	29,686	29,555	1,547	760	2,452		797	997	2,214	820	1,252
	6_G	402,966	402,981	402,974	402,978	402,970	402,967	402,967	403,071	403,070	29,461	29,156	29,127	1,128	1,213	2,101	797		606	2,227	1,190	1,671
	6_18	403,318	403,333	403,326	403,330	403,322	403,319	403,319	403,423	403,422	29,826	29,425	29,294	1,380	1,245	2,103	997	606		2,521	1,269	1,466
	6_F	403,762	403,776	403,769	403,773	403,765	403,762	403,762	403,866	403,865	30,652	30,749	30,102	2,084	2,132	3,602	2,214	2,227	2,521		1,875	2,738
	6_I	403,239	403,253	403,246	403,250	403,242	403,239	403,239	403,343	403,342	29,952	30,145	29,498	1,461	924	2,646	820	1,190	1,269	1,875		1,448
	6_J	403,517	403,532	403,525	403,529	403,521	403,518	403,518	403,622	403,621	29,949	29,710	29,579	1,683	1,038	2,394	1,252	1,671	1,466	2,738	1,448	

Figure S7. The number of interpopulation SNPs at different positions in the core genome alignment, for each of the three subseafloor populations. The gene annotations to the corresponding regions are shown.

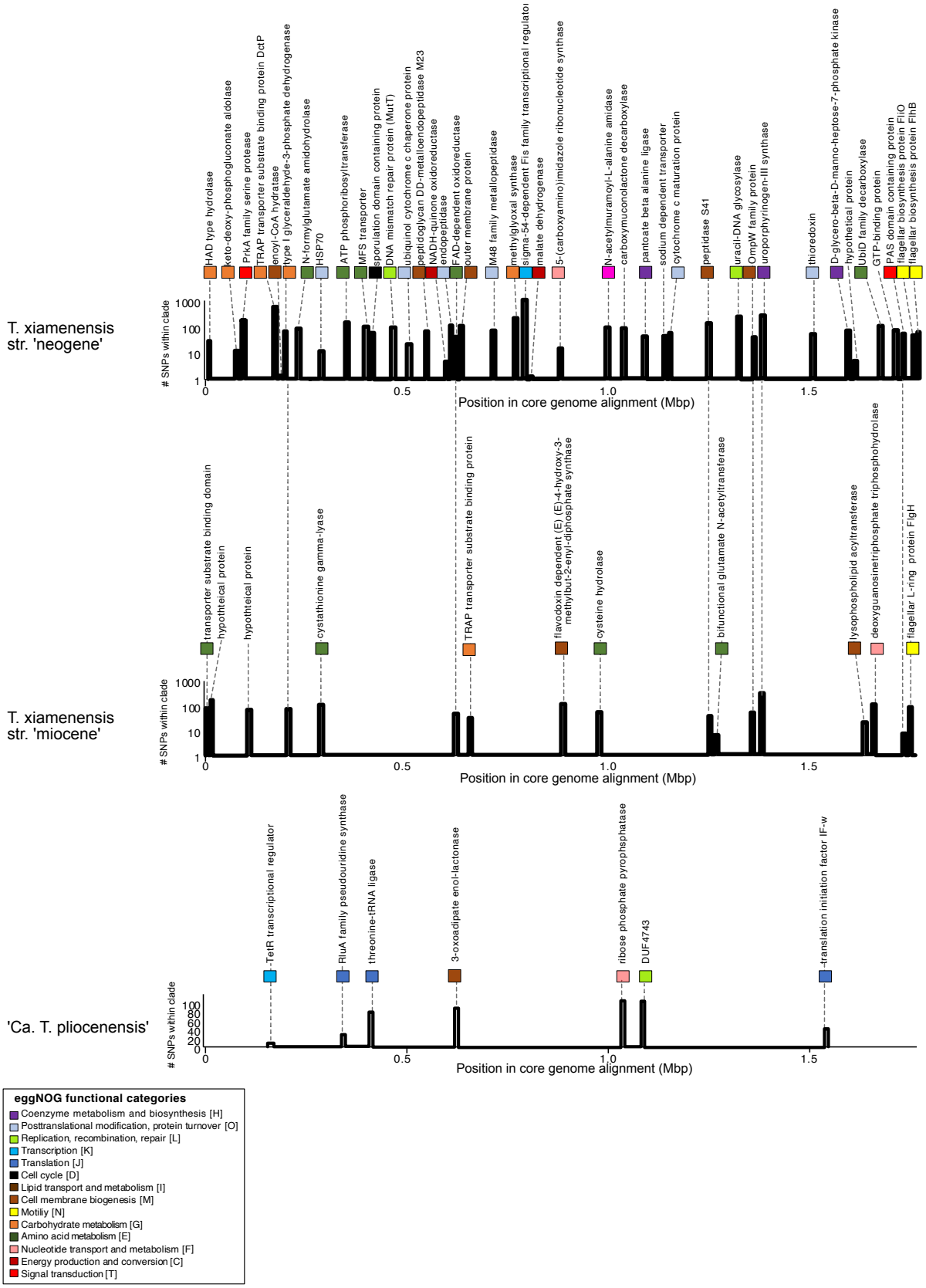

Figure S8: Interpopulation nucleotide diversity did not arise during laboratory cultivation. (A) Model of the number of mutations expected per genome (4.7 Mbp) as a function of total number of generations at five different mutation rates. Shading depicts the range of observed nucleotide diversity in subseafloor *Thalassospira* genomes (number of pairwise SNPs) as described in panel B. (B) The distribution of interpopulation nucleotide diversity. Points are the number of pairwise SNPs detected in subseafloor *Thalassospira* genomes. Box plots illustrate interquartile range ± 1.5 × interquartile range. The horizontal line in each box plot is the median.

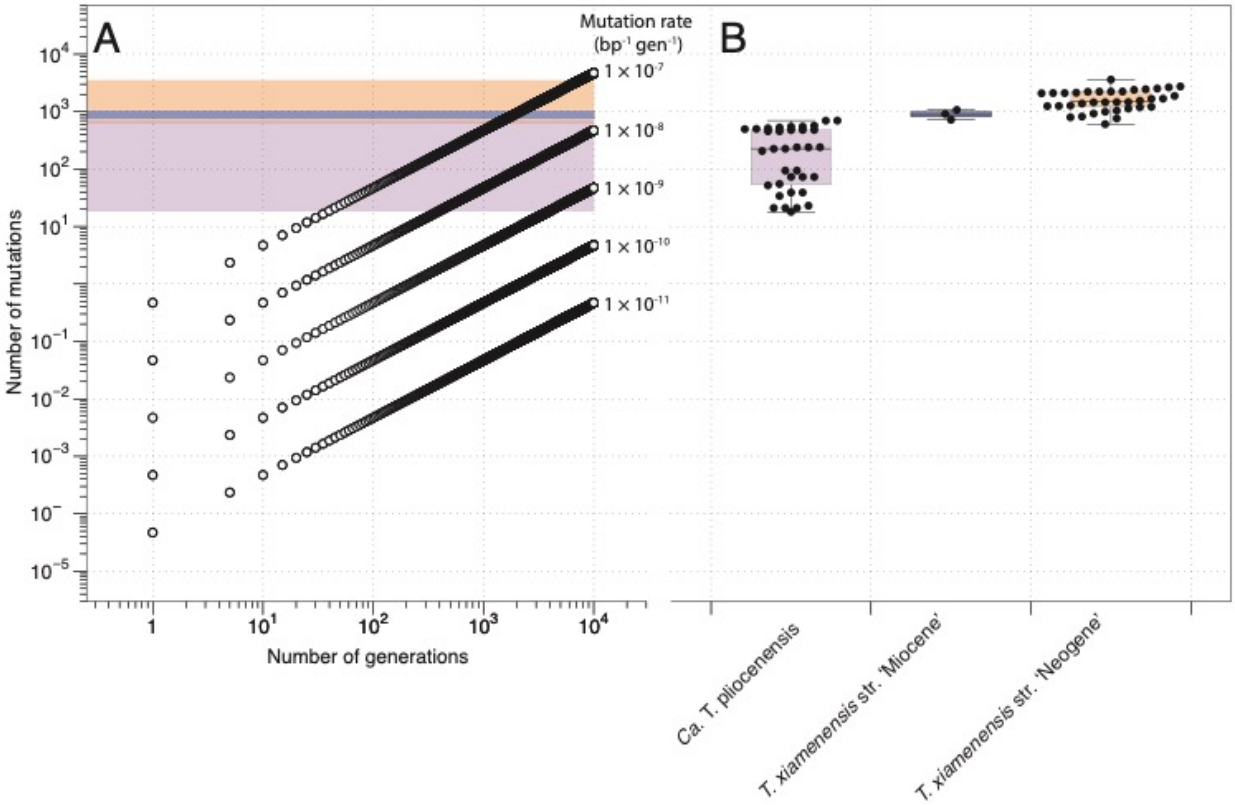

Figure S9: The heatmap shows the presence/absence of pseudogenes in the subseafloor genomes and the presence of these pseudogenes in type strains. Functional annotation (against eggNOG) of pseudogenes found in the subseafloor genomes only are compared to functional annotations of pseudogenes found in both the subseafloor and type strains.

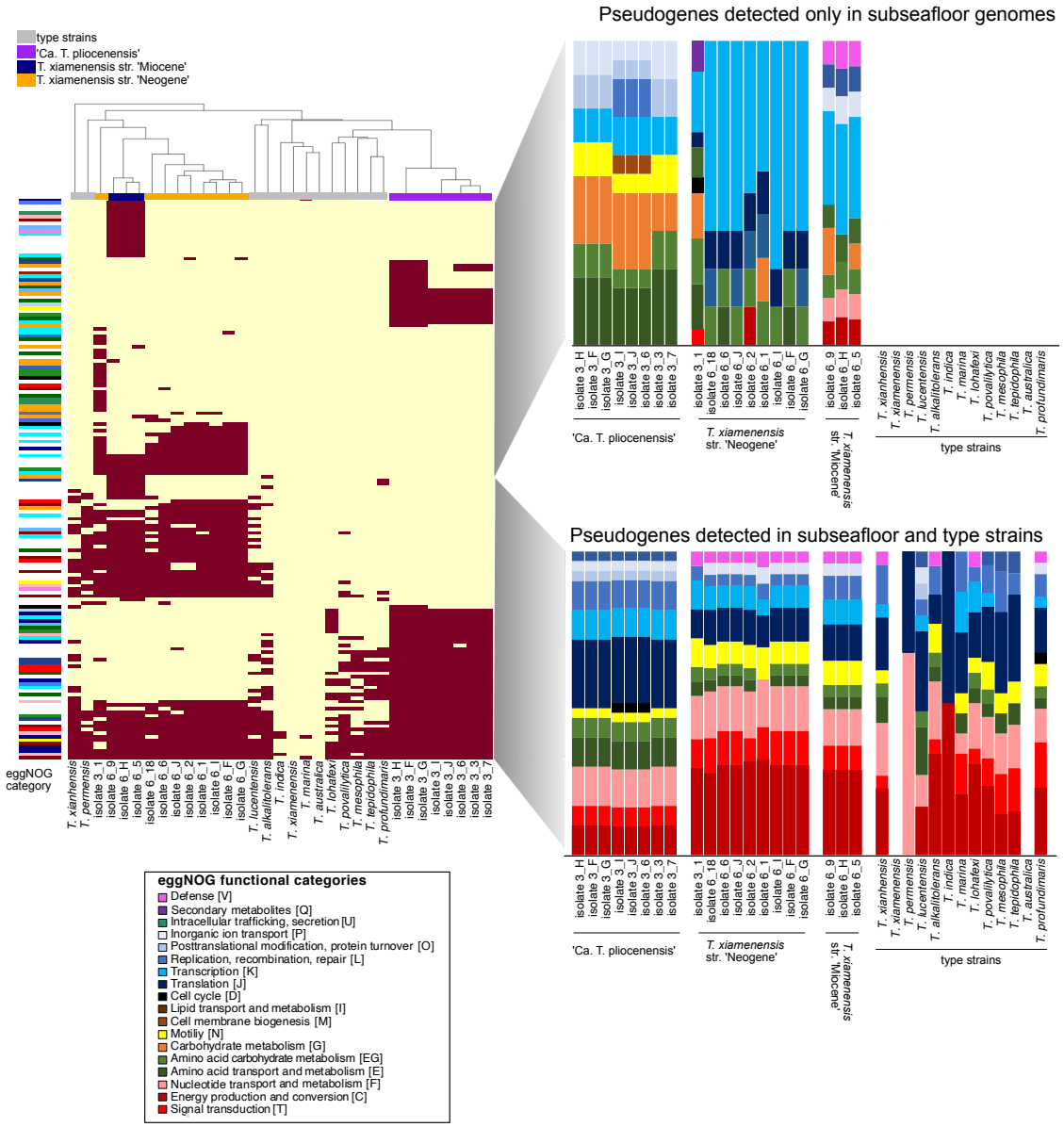

Figure S10: Histograms showing the average relative abundance of functional categories in pseudogenes found within each of the three subseafloor populations, compared to the type strains. The error bars represent standard deviations, and asterisks indicate functional categories of pseudogenes that were significantly higher in the subseafloor genomes compared to the type strain genomes (two sided T-Test, P<0.01).

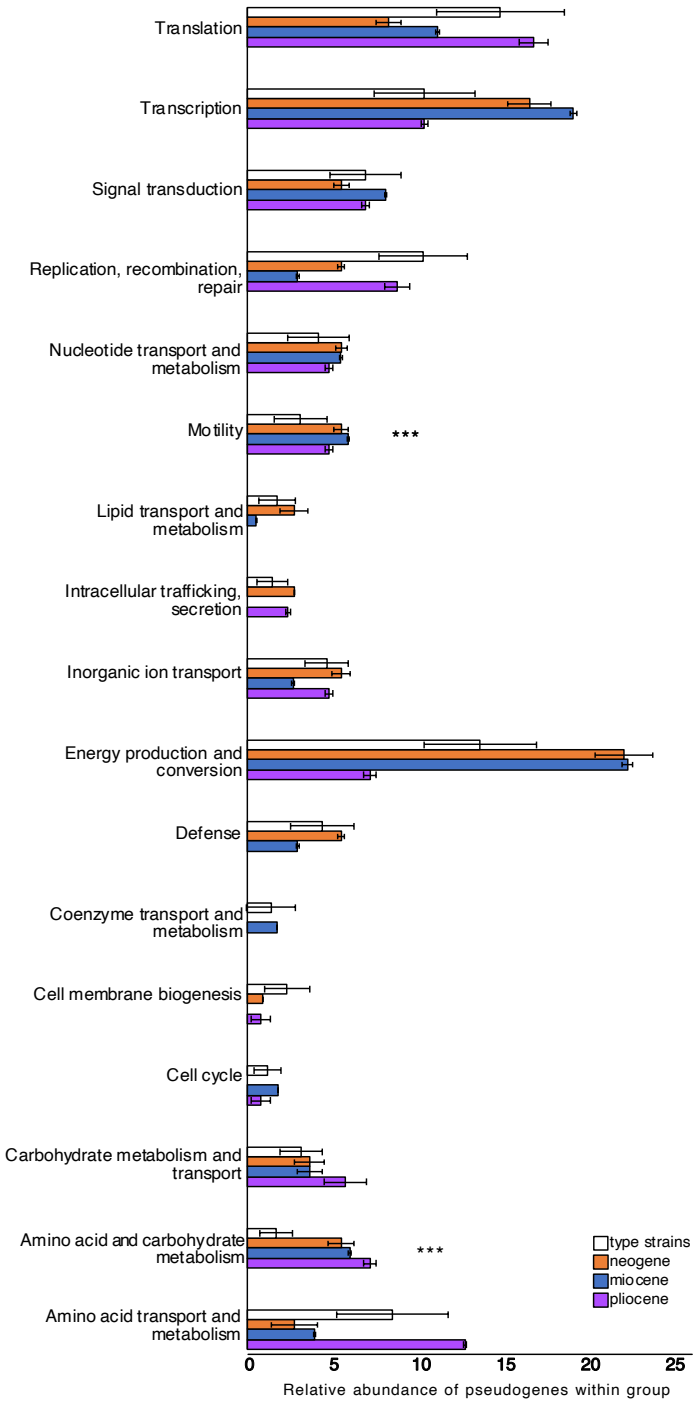

Materials and Methods

Sampling and pore water chemistry. All samples were taken during Expedition KN223 of the *R/V Knorr* in the North Atlantic, from 26 October to 3 December 2014. At site 11 (22°47.0′ N, 56°31.0′ W, water depth ~5600 m) via a long core piston-coring device (~28 m). Additional details of sampling are published elsewhere (*11, 13*). Dissolved oxygen concentrations in the core sections were measured with optical O_2 sensors from the equilibrated core sections and measured with needle-shaped optical O_2 sensors (optodes) (PreSens, Regensburg, Germany) as described previously (*11, 13*). The dissolved O_2 data from Expedition KN223 are archived and available online in the Integrated Earth Data Applications (IEDA) database (http://www.iedadata.org/doi?id=100519).

Physical sediment properties.

Deep-sea abyssal clay is characterized by very low permeability and extremely small pore diameter, despite its high porosity (*15*). Deep sea clay particles have a grain size of <0.2 µm, and the pore space between clay particles is smaller than a bacterial cell, limiting the movement of bacteria through pore space in the clay. Bioturbation can vertically redistribute cells within marine sediment, but bioturbation is restricted to the upper 0.5 meters of sediment (*31*) , and thus cannot vertically transport sediment surface material and microbes to depths of 3 and 6 mbsf. Considering the mean sedimentation rate of 1 m per million years, it can be concluded that the bacterial cultures obtained from sediment collected at 3 and 6 mbsf have been physically isolated from the surface world for millions of years.

DNA extraction, qPCR, 16S rRNA gene sequencing. DNA extractions, qPCR, and 16S rRNA gene sequencing were performed previously and described in Vuillemin et al (*12*). In brief, subcores were sampled aseptically with sterile syringes were subsampled aseptically in an ultraviolet (UV)–sterilized DNA/RNA clean HEPA- filtered laminar flow hood. DNA extraction was extracted from 10 g of sediment transferred into 50 ml of Lysing Matrix E tubes (MP Biomedicals) containing silica glass beads and homogenized for 40 s at 6 m/s using a FastPrep-24 5G homogenizer (MP Biomedicals) in the presence of 15 ml of preheated (65°C) sterile- filtered extraction buffer [76 volume % 1 M NaPO4 (pH 8), 15 vol- ume % 200 proof ethanol, 8 volume % MoBio's lysis buffer solution C1, and 1 volume % SDS]. The samples were incubated at 99°C for 2 min and frozen overnight at −20°C, thawed, and frozen again at −20°C overnight, followed by additional incubation at 99°C for 2 min and a second homogenization using the settings described above. After the second homogenization, the samples were centrifuged for 15 min, and the supernatants were concentrated to a volume of 100 ml using 50-kDa Amicon centrifugal filters (Millipore). Coextracted PCR-inhibiting humic acids and other compounds

632 were removed from the concentrated extract using the PowerClean Pro DNA Cleanup Kit (MoBio).
633 Extraction blanks were performed alongside the samples to assess laboratory contamination during the
634 extraction process.

635 DNA was quantified fluorometrically using a Qubit with a double- stranded DNA high-sensitivity
636 kit (Life Technologies). qPCR was performed using the custom primer dual indexed approach that tar-
637 gets the V4 hypervariable region of the 16S rRNA gene using updated 16S rRNA gene primers
638 515F/806R (515F, 5′-GTGYCAG- CMGCCGCGGTAA-3′; 806R, GGACTACNVGGGTWTCTAAT)
639 (*32*). Barcoded V4 hypervariable regions of amplified 16S rRNA genes were sequenced on an Illumina
640 MiniSeq following an established protocol (*33*). Bioinformatic processing of these previously published
641 sequence data is described by Vuillemin et al (*12*) in detail.

642

643 **Long term incubation set up.** Prior to setting up the incubations, the subcores were sampled with sterile
644 syringes using the sample aseptic technique used for the DNA extraction. For each sample depth, seven
645 grams of abyssal clay was placed into sterile 20-mL glass flasks and incubated with 4 mL of sterile
646 artificial seawater composed of either $H_2{}^{18}O$ (97% atomic enrichment) or unlabeled artificial seawater.
647 Vials were crimp sealed, with an oxygenated headspace of approximately 10 mL, and incubated at 8 °C.
648 The artificial seawater was different from the porewater at depth because there was no added nitrate, but
649 there was also no added ammonia which should be similar to the *in situ* conditions where ammonia is
650 generally below detection (*12*). Oxygen was measured continuously throughout the incubations using
651 non-invasive fiberoptic measurements as described previously (*12*). Small fluctuations in the oxygen
652 measurements in the killed control, and experimental incubations, were likely due to temperature
653 fluctuations of the incubator itself (±1˚C), since the non-invasive fiber optic oxygen sensor spots are
654 temperature sensitive (*12*). Oxygen consumption was detectable over 18 months in slurries consisting of
655 sediment and sterile artificial seawater (Fig S1), suggesting the presence of actively respiring microbes.
656 We used qSIP to measure the atom % ^{18}O-enrichment of actively growing microbial taxa
657 as described previously (*12*). In brief, after 7 and 18 months incubations DNA was extracted and
658 subjected to Cesium Chloride (CsCl) density gradient centrifugation. The same 16S 515F/806R
659 primers (described above) were used in qPCR (described above) to determine density shifts in
660 the peak DNA of buoyant density (BD) for each incubation. 16S rRNA gene amplicons from
661 each fraction resulting from the density gradient fractionation were Illumina sequenced as
662 described previously (*12*). To identify contaminants that may have entered during the

663 fractionation process, we also included in the sequencing run extraction blanks from the SIP
664 fractionation. OTUs containing sequences from extraction blanks were removed. Excess atm%
665 ^{18}O-enrichment was calculated for each OTU (including OTU6, corresponding to the subseafloor
666 *Thalassospira*) according to the equations for quantifying per OTU atomic enrichment.
667 The number of doublings for the *Thalassospira* OTU (OTU_6) detected at the 18 month
668 timepoint was calculated using qPCR normalized relative abundance of the 16S rRNA genes at
669 T0 and 18 months. The number of doublings was divided by the total number of days incubated
670 to calculate doubling times in days.
671
672 **Enrichments, cultivation, and sub-cultivation.** After the 18 months of incubation in sterile ^{18}O-labeled
673 artificial seawater, 25 µL of slurry was plated onto solid media (10 mg/mL yeast extract and 8 mg/mL
674 agar in artificial seawater [30 mM $MgCl_2 \cdot 6H_2O$, 16 mM $MgSO_4 \cdot 7H_2O$, 2 mM $NaCO_3$, 10 mM KCl, 9
675 mM $CaCl_2$, 450 mM NaCl)]), and after 2 days incubated in the dark at room temperature, abundant
676 colonies were observed growing on the surface of the petri dishes (Fig S1). No colonies were observed to
677 grow on control petri dishes that received 25 µL of ^{18}O-labeled artificial seawater slurry incubated for 18
678 months using starting material from autoclaved sediment (killed controls). This indicated that the colony-
679 forming bacteria were from the sediment and not contaminants introduced during the experimental set up
680 of the incubations. We attempted to culture chemoheterotrophic microbes directly from the collected
681 sediment samples using the same conditions, but no colony-forming units were observed on the petri
682 dishes, even after several months of incubation. Thus, long-term incubation of the sediment at 8 °C
683 simply in the presence of added water apparently stimulated the activity of many subseafloor bacteria to a
684 point at which they were able to grow on the surface of a petri dish.
685 Twelve colonies were picked from petri dishes containing colonies from the 3-mbsf and 6-mbsf
686 slurries. These colonies were streaked individually onto twelve separated new petri dishes, and a single
687 colony was picked from each of the twelve petri dishes (representing an original colony forming unit from
688 the enrichment) and grown in sterile liquid media (10 mg/mL yeast extract and 8 mg/mL agar in artificial
689 seawater [30 mM $MgCl_2 \cdot 6H_2O$, 16 mM $MgSO_4 \cdot 7H_2O$, 2 mM $NaCO_3$, 10 mM KCl, 9 mM $CaCl_2$, 450
690 mM NaCl)]). Single colonies were then grown up in liquid media. A portion of each of these colonies
691 was used for DNA extraction and genome sequencing, and the remaining volume was frozen as glycerol
692 stocks. Growth rates were determined in experiments with 20 mL crimp sealed glass flasks containing
693 0.1 mL of glycerol stock inoculated into 10 mL liquid media (10 mg/mL yeast extract in artificial
694 seawater [30 mM $MgCl_2 \cdot 6H_2O$, 16 mM $MgSO_4 \cdot 7H_2O$, 2 mM $NaCO_3$, 10 mM KCl, 9 mM $CaCl_2$, 450
695 mM NaCl)]) with 10 mL headspace, and gentle shaking. The optical density at 600 nm was measured

696 once every 30 minutes with a spectrophotometer, and growth rates were calculated from the exponential
697 phase. Under these conditions, growth rates of the subseafloor *Thalassospira* were similar across all three
698 clades and ranged from 0.064 to 0.31 h^{-1} (Fig. S5).
699
700 **Assessing the possibility for genome evolution during the 18 month enrichment.**
701 Because bacteria can evolve on lab experimental timescales (*5,6*) we considered the possibility that
702 all diversification and evolution happened during the 1.5 year enrichment. Using the qPCR-based estimate
703 for doubling time of the subseafloor *Thalassospira* OTU (OTU_6) in the incubation which was 36 (± 1.5)
704 days, the number of doublings with this rate over this time period would be approximately 15. According
705 to "Drake's rule (*20*), bacteria experience on average one mutation per 300 genomes replicated; thus, the
706 amount of nucleotide diversity (hundreds to thousands of mutations: Fig S8) that could be accumulated
707 during the incubation is insufficient to explain the observed divergence between the three subseafloor
708 populations. We thus conclude that the inter-population nucleotide diversity resulted from mutations that
709 were acquired after they were buried.
710
711 **Genome sequencing, de novo assembly, and annotation.** DNA was extracted from the isolates grown in
712 liquid culture until the end of exponential phase as described above. After reaching stationary phase,
713 cultures were pelleted via centrifugation and the supernatant was decanted. The cell pellets were
714 resuspended in a preheated (65°C) sterile filtered extraction buffer [76 volume % 1 M NaPO4 (pH 8), 15
715 volume %200 proof ethanol, 8 volume %MoBio lysis buffer solution C1,and 1 volume % SDS], and added
716 to lysing matrix E tubes (MP Biomedicals) containing silica glass beads and homogenized for 40 s at 6 m/s
717 using a FastPrep-24 5G homogenizer (MPBiomedicals). The samples were centrifuged for 15 min, and the
718 dissolved high molecular weight DNA in the supernatant was concentrated to a volume of 100 µL using
719 50-kDa Amicon centrifugal filters (Millipore). The concentrated extract was cleaned of proteins and other
720 non-genomic DNA organic matter using the PowerClean Pro DNA Cleanup Kit (MoBio). Extraction blanks
721 were performed alongside the samples to assess laboratory contamination during the extraction process.
722 Genomic libraries were prepared using the Nextera XT DNA Library Prep Kit (Illumina). Quality control
723 and quantification of the libraries were obtained on an Agilent 2100 Bioanalyzer System using the High
724 Sensitivity DNA reagents and DNA chips (Agilent Genomics). Metagenomic libraries were diluted to 1
725 nM using the Select-a-Size DNA Clean and Concentrator MagBead Kit (Zymo Research) and pooled for
726 further sequencing on the Illumina MiniSeq platform. Genomic libraries were sequenced to a depth of ca.
727 100x coverage using a high-output paired end 2 x 150 sequencing regent kit (Illumina).
728 In addition to Illumina sequencing, the high molecular weight genomic DNA was sequenced using the
729 NanoPore MinION. Sequencing libraries for the MinION were prepared using the Ligation Sequencing kit

730 (Oxford NanoPore Technologies), according to the manufacturers instructions. Barcoded libraries were
731 sequenced on the MinION using a Flongle R9 flow cell, base-called and demultiplexed using the MinIT
732 with ont-minit-release v19.12.5 and ont-guppy-for-minit v3.2.10 for base calling (Oxford NanoPore
733 Technologies).
734 A hybrid assembly was performed using both the short (Illumina) and long (NanoPore) read
735 sequencing data using Unicycler (v.0.4.0), which uses *de novo* assembled Illumina data from SPADES to
736 polish the *de novo* assembled contigs obtained from NanoPore data using RACON (*34*). The combined
737 assemblies of Illumina and NanoPore data resulted in a relative low number of contigs (9-12 per genome),
738 and a predicted genome completeness of 100% of nearly all genomes (Table S1). Genome completeness
739 was determined using CheckM (*35*). Genomes were annotated using RASTk (*36*).
740
741 **Core genome phylogenetic analyses.** The core genome was defined as the set of orthologous
742 genes which were shared in all subseafloor and extant *Thalassospira* genomes. Orthologous genes were
743 defined as those sharing >30% amino acid similarity to the collective suite of genes encoded within the
744 type strain *Thalassospira xiamenensis* M-5. *T. xiamenensis* M-5 was chosen as the reference genome for
745 this purpose, because it is the only publicly available genome of a cultivated *Thalassospira* isolate that is
746 completely closed and represents a single chromosome and a 190 Kb plasmid (*14*). A total of 1,809
747 orthologous genes were identified that are encoded by all *Thalassospira* strains that had >30% sequence
748 similarity to genes encoded within the *T. xiamenensis* M-5 genome. Each of these 1,809 genes was
749 individually aligned between all *Thalassospira* strains using MUSCLE (*37*), and the individual 1,809
750 alignments were then concatenated into a single core genome alignment for the subsequent phylogenomic
751 analysis (ClonalFrameML, HyPhy, aBRSEL) using Geneious Prime (version 2019.2.1). After
752 concatenation of all core genes, the total size of the core genome alignment was 1,817,073 nucleotide
753 characters, and 34 taxa (21 subseafloor strains, and 13 type strain taxa). A Maximum-Likelihood phylogeny
754 was created using PhyML (*38*) with a GTR model of evolution and 100 bootstrap replicates, which was
755 implemented within SeaView (*39*). The resulting phylogenetic tree and the concatenated core genome
756 alignment were used as inputs for subsequent ClonalFrameML and dN/dS analyses.
757 The contributions of mutations and recombination to the genomic diversity in the concatenated core
758 genome alignment, the number of recombination events (imports) per genome, and the positions of
759 recombination hot spots, were investigated using ClonalFrameML (*19*). Nucleotides unaffected by
760 recombination are referred to as unimported and nucleotides subject to recombination are referred to as
761 imported (*19*). ClonalFrameML provides the relative rate of recombination to mutation (R/Theta), the mean
762 length of recombined DNA (Delta), and the mean divergence of imported DNA (Nu). These results were
763 used to calculate the relative contribution of recombination versus mutation to the overall genomic diversity

764 (r/m), using the formula r/m = (R/Theta) * Delta * Nu. ClonalFrameML was performed in three separate
765 runs, respectively containing a core genome alignment that contained (1) all genomes, (2) only the
766 subseafloor genomes, and (3) only the type strains. The resulting r/m values from these three groups
767 (presented in Table 1) were then used to interpret the relative importance of mutations compared to
768 recombination, in the separate groups (e.g., type strains versus subseafloor strains).
769 In addition to calculating sites and rates of recombination in the core genome, ClonalFrameML
770 also estimates the ancestral sequences at internal nodes of the clonal genealogy, and any missing base calls
771 in the observed sequences. The reconstruction of ancestral sequence states is performed using maximum
772 likelihood and the ClonalFrame model can be thought of as a hidden Markov model (HMM) when the
773 ancestral and descendant genomes for each branch of the clonal genealogy have been observed or
774 reconstructed (*19*). The hidden state of the HMM records whether each nucleotide was subject to
775 recombination or not on the branch connecting the two genomes. We acknowledge that drawing inference
776 under the resulting ancestral recombination graph is a notoriously complex statistical problem (*19*). Instead,
777 here we use ClonalFrameML only to assess within-group recombination (e.g., between species within the
778 genus *Thalassospira*), and thus our analysis cannot assess the influence of external recombination (from
779 species outside the genus *Thalassospira*).
780 The ratio of non-synonymous (dN) to synonymous (dS) mutations in the core genome alignment
781 (global ω ratio) was estimated using HyPhy v2.2.4 (*40*), and applying the adaptive branch-site random-
782 effects likelihood (aBSREL) approach (*41*) to all branches in all subfamilies. Because of the high similarity
783 of the subseafloor genomes, aBSREL was run multiple times using the core genome alignment with only
784 one representative of the nearly identical subseafloor genomes included in each separate run. For each of
785 these runs, one representative genome of *T. xiamenensis* strain 'Neogene', *T xiamenensis* strain 'Miocene,
786 and 'Ca. *T. pliocenensis*' were included together with all other *Thalassospira* type strain genomes in each
787 aBSREL run. Then, the aBSREL run was repeated with the same type strains but different subseafloor
788 genomes from those same three clades, until dN/dS estimates were obtained for all subseafloor genomes.
789
790 **Pangenome analysis.** All subseafloor and extant *Thalassospira* genomes were analyzed in Anvi'o v6.2
791 using pangenome workflow (*42*). Briefly, each genome was converted into an anvi'o contigs database.
792 Genes were functionally annotated using eggnog v5.0 (*43*) with eggNOG-mapper (*44*) and imported back
793 to each genome's anvi'o contig database. Genome storages were generated using 'anvi-gen-genomes-
794 storages' and 'anvi-pan-genome' was deployed with parameters '--min-bit 0.5' (*45*), '--mcl-inflation' 10
795 (*46*), and the flag '--use-ncbi-blast' (*47*). The anvi'o pan database and summary of gene clusters stored in
796 FIGshare (https://figshare.com/s/06ba1287a00ab01a1ee).
797

Identifying pseudogenes. We estimated the number of pseudogenes within the genomes using two programs, Psi-Phi (*48*) and DFAST (*49*). Psi-Phi uses a conservative criterion considering a pseudogene only when it lost >20% of its original length, and enhances pseudogene recognition among closely related strains both in annotated regions by identifying incorrectly annotated open reading frames (ORFs) and in intergenic regions by detecting new pseudogenes (*48*). Psi-Phi classifies pseudogenes as either identified pseudogenes and those as being possible, but potentially not pseudogenes. To be conservative, we only considered genes identified as pseudogenes from Psi-Phi and did not consider those flagged as 'potential pseudogenes'. As a second check of pseudogene content, we searched genomes for pseudogenes using DFAST (*49*). The estimated number of pseudogenes per genome was then taken as an average of the numbers detected both using both methods (Psi-Phi and DFAST). On average, Psi-Phi identified a higher number of pseudogenes per genome (57 ±10) compared to DFAST (32 ±4), but the variation between methods for the same genome was consistent (average variation =27, standard deviation of averages = 7). This minimal variation between individual genomes indicates that biases inherent to the pseudogene prediction methods affected the different genomes equally, and thus allow for a pseudogene comparison between the genomes.

Supplemental references

31. L. R. Teal, M. T. Bulling, E. R. Parker, M. Solan, Global patterns of bioturbation intensity and mixed depth of marine soft sediments. *Aquatic Biology* **2**, 207-218 (2008)
32. A. E. Parada, D. M. Needham, J. A. Fuhrman, Every base matters: assessing small subunit rRNA primers for marine microbiomes with mock communities, time series and global field samples. *Environ Microbiol* **18**, 1403-1414 (2016).
33. M. Pichler *et al.*, A 16S rRNA gene sequencing and analysis protocol for the Illumina MiniSeq platform. *Microbiologyopen*, e00611 (2018).
34. R. R. Wick, L. M. Judd, C. L. Gorrie, K. E. Holt, Unicycler: Resolving bacterial genome assemblies from short and long sequencing reads. *PLoS Comput Biol* **13**, e1005595 (2017).
35. D. H. Parks, M. Imelfort, C. T. Skennerton, P. Hugenholtz, G. W. Tyson, CheckM: assessing the quality of microbial genomes recovered from isolates, single cells, and metagenomes. *Genome Res* **25**, 1043-1055 (2015).
36. R. Overbeek *et al.*, The SEED and the Rapid Annotation of microbial genomes using Subsystems Technology (RAST). *Nucleic Acids Res* **42**, D206-214 (2014).
37. R. C. Edgar, MUSCLE: multiple sequence alignment with high accuracy and high throughput. *Nulceic Acids Res* **32**, 1792-1797 (2004).

835 38. S. Guindon, F. Lethiec, P. Duroux, O. Gascuel, PHYML Online--a web server for fast
836 maximum likelihood-based phylogenetic inference. *Nucleic Acids Res* **33**, W557-559
837 (2005).
838 39. M. Gouy, S. Guindon, O. Gascuel, SeaView version 4: A multiplatform graphical user
839 interface for sequence alignment and phylogenetic tree building. *Mol Biol Evol* **27**, 221-
840 224.
841 40. S. L. Pond, S. D. Frost, S. V. Muse, HyPhy: hypothesis testing using phylogenies.
842 *Bioinformatics* **21**, 676-679 (2005).
843 41. M. D. Smith *et al.*, Less is more: an adaptive branch-site random effects model for
844 efficient detection of episodic diversifying selection. *Mol Biol Evol* **32**, 1342-1353 (2015).
845 42. A. M. Eren *et a*l., Anvi'o: an advanced analysis and visualization platform for 'omics data.
846 *PeerJ* **3**, e1319 (2015).
847 43. J. Huerta-Cepas *et a*l., eggNOG 5.0: a hierarchical, functionally and phylogenetically
848 annotated orthology resource based on 5090 organisms and 2502 viruses. *Nucleic Acids*
849 *Res* **47**, D209-D314 (2018).
850 44. J. Huerta-Cepas *et a*l., Fast Genome-Wide Functional Annotation through Orthology
851 Assignment by eggNOG-Mapper. *Mol Biol Evol* **34**, 2115-2122 (2017).
852 45. M. N. Benedict et al., ITEP: and integrated toolkit for exploration of microbial pan-
853 genomes. *BMC Genomics* **15**, 12.1186/1471-2164-15-8 (2014).
854 46. S. van Dongen, C. Abreu-Goodger, Using MCL to extract clusters from networks. In
855 "Bacterial Molecular Networks: Methods and Protocols" Eds. J. van Helden, A.
856 Toussaint, D. Thieffry. Springer New York, New York, NY. Pages 281-295.
857 47. S. F. Altschul *et al.,* Basic local alignment search tool*. J Mol Biol* **215**, 403-410 (1990).
858 48. E. Lerat, H. Ochman, Psi-Phi: exploring the outer limits of bacterial pseudogenes.
859 *Genome Res* **14**, 2273-2278 (2004).
860 49. Y. Tanizawa, T. Fujisawa, Y. Nakamura, DFAST: a flexible prokaryotic genome annotation
861 pipeline for faster genome publication. *Bioinformatics* **34**, 1037-1039 (2018).
862

863